Research Square

Preprints are preliminary reports that have not undergone peer review.
They should not be considered conclusive, used to inform clinical practice,
or referenced by the media as validated information.

# Assessment of HyperSight Cone-Beam CT for Dose Calculation in External Regulatory Audit Conditions

**Peter Toth**

Peter.Toth@icon.team

ICON Cancer Centre

**Maddison Shaw**

ICON Cancer Centre

**Andrew Alves**

Australian Radiation Protection and Nuclear Safety Agency

**Peter Phung**

ICON Cancer Centre

**Ben Archibald-Heeren**

ICON Cancer Centre

**Research Article**

**Keywords:** Cone-beam CT, HyperSight, adaptive radiotherapy, dosimetry audit

**Posted Date:** July 16th, 2026

**DOI:** https://doi.org/10.21203/rs.3.rs-10261946/v1

**License:** This work is licensed under a Creative Commons Attribution 4.0 International License.
Read Full License

**Additional Declarations:** No competing interests reported.

## Abstract

# Background

Cone-beam computed tomography (CBCT) is increasingly being integrated into adaptive radiotherapy workflows; however, its use for accurate dose calculation has historically been limited by image quality and Hounsfield unit inconsistencies. The introduction of advanced CBCT systems such as HyperSight aims to improve CT number accuracy and consistency and enable more reliable dose calculation directly on CBCT datasets. Independent validation using clinically relevant audit frameworks is therefore essential to assess its suitability for treatment planning and adaptive applications.

# Purpose

This study aimed to evaluate the feasibility of HyperSight cone-beam CT (CBCT) for radiotherapy treatment planning by assessing its ability to meet the Australian Radiation Protection and Nuclear Safety Agency (ARPANSA) Level III independent dosimetry audit requirements. A secondary aim was to compare HyperSight-based audit outcomes with seven non-HyperSight Halcyon Level III audit results acquired across the author's clinical network between 2021 and 2023.

# Methods

CBCT-based treatment plans were generated across three planning categories of increasing complexity and submitted for Level III external dosimetry audit. Dosimetric agreement between CBCT-based and fan-beam CT (FBCT)-based plans was evaluated, and HyperSight audit results were compared with historical non-HyperSight Halcyon audit performance where available.

# Results

CBCT-based plans met Level III audit criteria for conformal and modulated plan groups, while the lung SBRT case failed in both audit sessions. HyperSight audit outcomes were comparable to historical non-HyperSight Halcyon results across the ICON network, with no clinically significant degradation in dose delivery accuracy observed.

# Conclusion

HyperSight CBCT-based planning can achieve Level III audit compliance comparable to FBCT-based approaches; however, implementation in stereotactic body radiotherapy (SBRT) planning should be undertaken with extreme caution due to the higher sensitivity of complex dose distributions to imaging and calculation uncertainties.

# Introduction

In an ideal scenario, a patient undergoing conventional radiotherapy would present for daily treatment in the same anatomical setup as their planning CT scan. In clinical practice, due to patient anatomical changes or minor setup variations, there may be divergence between the planned and delivered dose. Adaptive treatment techniques seek to address this challenge by using images throughout the treatment course to assess and, where necessary, adjust the patient treatment plan to better align with the initial clinical intent. Adaptation can be performed in real-time, on a per fraction basis (online) or over the course of treatment (offline) with each approach demonstrating the potential to improve overall clinical planning metrics as outlined by Lu et al [1].

Research into the use of on-board cone-beam computed tomography (CBCT) imaging for adaptive radiation therapy continues to advance, supported by the emergence of several commercial solutions (e.g., Radformation, SeeTreat and TheraPanacea) [2–4]. While some success on the software side has been demonstrated in specific patient geometries outlined by Hu et al. [5], most current approaches avoid direct dose calculation on CBCT images due to limitations such as Hounsfield unit (HU) instability, image truncation, and degraded image quality caused by variable scatter conditions.

To overcome these challenges Robar et al. [6] explored various techniques, including the generation of synthetic CT images via artificial intelligence or deformable image registration, as well as the application of bulk density overrides. Although these methods can improve dose calculation accuracy, they introduce additional steps and uncertainties into the adaptive workflow. This added complexity increases the demands on quality assurance and prolongs processing times, potentially limiting clinical efficiency.

Over the past two years, an innovative clinical on-board imaging system, Varian's HyperSight solution, has demonstrated significant improvements in on-board radiotherapy image quality. The advanced imaging system features upgraded hardware, including a large flat-panel detector (86 × 43 cm on Halcyon; 43 × 43 cm on TrueBeam), and enhanced software reconstruction algorithms such as iCBCT Acuros and iCBCT MAR reconstructions [6, 7]. Multiple studies have evaluated HyperSight CBCT on the Halcyon platform, demonstrating image quality comparable to an image set acquired using conventional CT (FBCT). Key image quality metrics, that are vital for treatment planning, including contrast-to-noise ratio, artifact reduction, image uniformity, and Hounsfield unit (HU) accuracy, have shown strong alignment between HyperSight CBCT and FBCT [6–10]. Furthermore, findings suggest that HyperSight images are suitable for direct dose calculation, with appropriate considerations. Haertter et al. [11] have compared the HyperSight CBCT image quality to a FBCT and obtained the American College of Radiology Program accreditation, MacDonald et al. [9] have proved the HyperSight CBCT is suitable for treatment planning and dose calculation, passing the Imaging and Radiation Oncology Core’s external audit program of dosimetry.

Studies of Robar et al. [6] and Zhao et al. [12] observed that respiratory motion significantly degrades image quality. Kunnen et al. [13] focused on specific anatomical sites, whilst MacDonald et al. [9] has

explored its application in urgent palliative cases. These findings suggest that while the HyperSight system is not yet without limitations, it remains a viable option for treatment planning and delivery with appropriate considerations.

In Australia, the implementation of new radiation therapy technologies requires external auditing before clinical introduction. The Australian Radiation Protection and Nuclear Safety Agency (ARPANSA) offers the Australian Clinical Dosimetry Service (ACDS) audit program, which operates across three levels [14]. The Level III audit evaluates the accuracy of dose delivery in a simulated patient scenario within a radiation therapy facility. This end-to-end assessment replicates all clinical steps a patient would undergo during treatment, ensuring comprehensive quality assurance. This involves using an anthropomorphic thorax phantom (CIRS Inc.; Norfolk, VA, USA) [15]. It comprises of water equivalent plastic body (ρ: 1.04 g/cm³), inhale lung regions (ρ: 0.21 g/cm³) with a spherical 2 cm lung tumour (ρ: 1.06 g/cm³) in the right lung, and an anatomically correct spine composed of cortical (ρ: 1.91 g/cm³) and trabecular (ρ: 1.20 g/cm³) bone equivalent materials. It is used for the full treatment process intended for radical therapy. The audit assesses multiple treatment techniques and planning calculation algorithms. Dosimetry verification is conducted using ionization chambers (for 3DCRT, IMRT, VMAT), radiochromic film, and microDiamond detectors (for SBRT).

It was hypothesised that the improved image quality provided by the HyperSight imaging system would enable successful completion of the national audit using CBCT-acquired simulation scans.

This hypothesis was tested by performing the national audit in parallel with conventional FBCT simulation and comparing audit results to historic measurements across seven Halcyon national audits.

The aim of this study was to assess the feasibility of passing the ARPANSA Level III audit using HyperSight CBCT images for treatment planning, similarly to the approach reported by Haertter et al. [11] within the American College of Radiology accreditation program. In addition, dosimetric differences between CBCT-based and FBCT-based treatment plans were evaluated. As an extension of this work, the HyperSight audit results were also compared with the authors' previously completed Level III audit results from seven non-HyperSight Halcyon systems.

# Methods

The ACDS Level III audit was performed at our facility on a Varian Halcyon Model 4.1 with HyperSight capability. A provided anthropomorphic thorax phantom was simulated with the HyperSight CBCT system on a Halcyon v4.1 linac [Varian Medical Systems, Siemens Healthineers, Palo Alto, CA, USA] as per the ACDS protocol and guidelines. Acquisitions were taken with 1 mm and 2 mm reconstructed slice thickness with the iCBCT Acuros algorithm [15]. Immediately following the HyperSight simulation, the phantom was scanned on a Siemens Somatom Definition Flash FBCT [Siemens Healthineers, Erlangen, Germany]. The image acquisition parameters are summarised in Table 1.

Table 1
Acquisition parameters for FBCT and HyperSight CBCT

| **CTDIvol [mGy]** | **Siemens Somatom Definition FBCT** | **Varian HyperSight CBCT** |
|---|---|---|
| | **1.35** | **13.271** |
| Diameter [mm] | 500 | 537.47 |
| X-ray tube voltage [kV] | 120 | 125 |
| Tube current [mA] | 32 | 119 |
| Exposure time [ms] | 500 | 5820 |
| Total exposure [mAs] | 20 | 698 |
| Reconstruction algorithm | Convolution Kernel: B31f | Thorax iCBCT Acuros 2.0 |

The template structure sets were provided by ACDS and registered to the iCBCT and FBCT images, with structures copied between scans for consistency.

## Planning Process

The ACDS Level III audit utilizes 12 predefined cases (A-L). Case H is no longer used within the current protocol. Case I was not relevant to this audit and was therefore excluded from analysis, resulting in 10 evaluated cases (A-D, E-G and J-L). These cases applied to a standard anthropomorphic phantom for audit with associated structures sets to evaluate various treatment modalities. These cases can be divided to three sections, A-D, E-G, and J-L, as outlined in Table 2 and more information about the field alignment is available at appendix Table A1. Case K was calculated with the AAA algorithm; however, as AXB is used clinically, it is reported for completeness but is not relevant to the audit outcome.

Table 2
Plan, Phantom and Measurement Setup for Audit cases [14, 17, 19, 20]

| | Case | Description and Field alignment | Measurement points and chamber type |
|---|---|---|---|
| Section 1<br><br>3D Conformal Radiation Therapy (3DCRT) audit cases [14] | A | Detecting gross errors in treatment planning and experimental setup.<br><br>**AP**<br><br>Calculated two plans with AAA and AXB algorithm[13] | 2<br><br>Farmer chamber |
| | B | Verifying dose calculations using dynamic flattening for the FFF beam.<br><br>**RLAT - AP - LLAT** | |
| | C | Assessing dose accuracy at multiple points behind a lung inhomogeneity.<br><br>**LLAT** | |
| | D | Evaluating dose calculations at various points behind a lung inhomogeneity with dynamically flattened FFF field.<br><br>**LLAT** | |
| Section 2<br><br>IMRT/VMAT audit cases [14] | E | Verifying dose accuracy for a C-shaped target volume surrounding a central avoidance structure.<br><br>**VMAT** | 7<br><br>CC13 chamber |
| | F | Assessing dose delivery to the same C-shaped target in the presence of tissue inhomogeneities.<br><br>**VMAT** | |
| | G | Evaluating dose accuracy in a complex scenario involving two target volumes with distinct dose objectives and an exclusion volume fully encompassed by the higher dose target volume.<br><br>**VMAT** | |
| Section 3<br><br>SBRT audit cases [19] | J | Assessing dose delivery to a very simple SBRT target.<br><br>**VMAT** | 1<br><br>microDiamond detector and Gafchromic film |

| | | | |
|---|---|---|---|
| | K | Evaluating the accuracy of dose delivery to a SBRT spine (complex) target.<br><br>**VMAT**<br><br>Calculated two plans with AAA and AXB algorithm | 1<br><br>microDiamond detector and Gafchromic film |
| | L | Verifying the accuracy of the delivery of dose to a SBRT Lung target without motion management.<br><br>**VMAT** | 1<br><br>microDiamond and Gafchromic film |

Ten cases of various treatment modalities were planned in accordance with the provided ACDS audit instructions. Planning was conducted on the HyperSight CBCT with Eclipse v18, calculated with dose to medium using AXB v16.1 and AAA v16.1 for certain cases. All plans met with the auditor's criteria on review.

Following initial CBCT-based planning, each plan was copied over to the FBCT through a 3D rigid registration and recalculated with fixed MUs ensuring consistent planning dosimetry between the image sets.

Patient specific quality assurance (PSQA) was performed on all delivered plans as per the department protocol. PSQA included portal dosimetry and secondary 3D dose calculation. All plans passed local QA tolerances prior to inclusion in the study.

During the audit, our facility provided the planned dose values based on HyperSight CBCT datasets (Data A) to ACDS which were then compared to the measured dose values. Plan reports, 3D plan dosimetry and QA results were provided to ACDS for review prior to the on-site audit. The planned dose values were also collected from the FBCT plans (Data B) for comparison but not provided to the auditors for evaluation.

# Audit Measurement

Audit measurements were performed with the scanned phantom, the auditor's independent condition (thermometer, and barometer) and dosimetry equipment. The machine's output was verified within a tolerance of ± 1% by the site physicist before the audit.

All plans were delivered following the same setup and imaging processes undertaken for clinical treatment. A Radiation Therapist performed a treatment check, applied clinical setup, and completed the image guided radiation therapy (IGRT) process. All plans were delivered to multiple ion chambers, with secondary standard calibrations, inserted into the anthropomorphic phantom. Measurements were completed with detectors (ion chambers, microDiamond detectors and Gafchromic film) as per Table 2. All measurement methods were independently calibrated for dose to water. To ensure accurate comparison with calculated dose, detector measurements were converted to dose to medium using

correction factors outlined by AAPM TG-329 [18]. The SBRT plans (Cases J-L) were delivered to Gafchromic film for spatial and dosimetric accuracy, with a microDiamond detector also used to measure point dose [19].

All measurements were performed independently from facility staff, as external audit personnel attended to this task.

In addition to the performed audit, retrospective audit reports from the institution were collected for comparison of HyperSight simulation against a distribution of Halcyon sites. In total seven Halcyon linac audits were relevant to the study, including a prior audit at the study site and 6 additional centres within the institution. Due to variations in commissioned techniques not all audit cases were performed at all sites. Included results are provided where AXB was utilised for calculation in the audit case. Case K, which simulates spine SBRT, is only planned with the AAA dose-calculation algorithm at the institution, and as such was excluded from the historic analysis.

Analysis

Analysis and results for the audit were provided independently by the ACDS auditors. Provided audit results include comparison of independently measured dose to the facility stated plan dose [14, 16]. For chamber measurements, audit tolerances are set at +/-3.3%, +/- 5% and > +/-5% for Optimal (O), passed at Action (A) Out of Tolerance (OT) levels respectively.

In this paper, the authors formalise dose variation as positive where measurement is greater than calculated dose. It should be noted that, in ACD reporting, the inverse conversion is used: a negative variation indicates where ACDS measures greater than the facility states (i.e. variation = (planned/measured)-1). This clarification is key if comparing results in this paper to reports from ACDS at the readers departments. The ACDS also provide information how results correspond to the average of results across Australian departments [14]. In addition to chamber/detector dose variation the audit report included gamma analysis for SBRT cases measured with film dosimetry. The gamma [γ] criteria of 5%/2 mm relative to the prescription dose in each case, with dose < 10% suppressed, is used. The outcome is determined from the percentage of points where $\gamma \leq 1$. A case is considered passed at the Optimal level (O) if ≥ 95% of points meet $\gamma \leq 1$. It is considered a pass at Action level (A) if ≥ 90% and < 95% of points meet $\gamma \leq 1$. If < 90% of points meet $\gamma \leq 1$, it is considered Out of Tolerance (OT) [14, 20].

Initial audit results, performed in January 2025, incurred SBRT measurements with Action or Out-of-Tolerance results. Subsequent investigations were performed, and a subset of cases were re-measured in a follow-up investigation in May 2025. Results from both audits are included in the analysis results.

# Results

Part 1

The results of the first and second audit are provided in Fig. 1, and in tabulated data in Table A2 of the appendix.

The linac output was measured as 0.6% high on the day of the first audit in January 2025. As some results measured high (with Passed at Action or Out-of-Tolerance levels), a second audit was performed following another absolute calibration, where the machine output was registered as -1.0% prior to the audit. The subset of measurements performed in this audit (Cases A, E–G, and L) incorporate this dose offset.

Chamber measurement variation is reported for both the HyperSight simulation plan and the recalculated plans on the FBCT in Table A3 of the appendix. Measurements between the FBCT and HyperSight results are common, as is the phantom imaging setup. Variation between results is therefore isolated to dose plan calculation differences owing to the imaging systems. Average variation and standard deviation in measurement from calculated planned chamber doses were − 1.0% ±1.2% and − 0.8% ±1.3% for the HyperSight and FBCT calculations respectively.

In addition to the chamber dose variations provided in Fig. 1, Gafchromic film results are provided for both audits (where relevant) in Table 3 that reached Action and Out-of-Tolerance levels:

Table 3
Gafchromic film results

| Case | Field | Path | DTA (70% iso) L-R (mm) | DTA (70% iso) A-P (mm) | DTA (70% iso) S-I (mm) | Gamma Analysis (5%/2 mm) | ROI 90% Dose Variation (%) | Outcome |
|---|---|---|---|---|---|---|---|---|
| J | SBRT | Tissue | -0.5 | -0.1 | Not Scored | 91.2 | -9.2 | PASS-REVIEW |
| K | SBRT | Spine | 1 | Not Scored | Not Scored | 91 | Not Reported | PASS-REVIEW |
| L | SBRT | Lung | Not Scored | Not Scored | -0.2 | 82.9 | -7.4 | Out of Tolerance |
| L Second Audit | SBRT | Lung | Not Scored | Not Scored | -0.4 | 89.3 | -5.6 | Out of Tolerance |

Of the 10 cases, both the HyperSight and the FBCT recorded 9 Optimal or Passed at Action results with the lung SBRT case remaining Out of Tolerance in both audit sessions.

Part 2

Results from institutions historic audits are provided in Fig. 2 and Table A3 in the appendix.

All sites, historic and HyperSight, performed the audit with the same instructions. Individual plans were created at participating sites to meet these requirements. The resultant plans are therefore similar but

differ in optimisation solution, and final delivery sequence. To account for this variance, comparison is performed between local measured percentage variance, not absolute dose values. For each case, the relative dose difference from these audits were compared to the HyperSight audit result, enabling a direct assessment of dosimetric consistency across the platforms.

The adjusted variations of each case with the output of the day before the audit are presented in appendix Table A3.

Table 4
Cases average Vs HyperSight

| **Case A Pt 1** | **Average of the 7 linacs** | **SD for all 7 linacs** | **HyperSight combined results, from the second audit where applicable** | **Difference between the average of the 7 Linacs and the HyperSight combined results** |
|---|---|---|---|---|
| | **0.01** | **0.46** | **-0.54** | **-0.56** |
| Case A Pt 10 | 0.64 | 1.03 | 0.07 | -0.58 |
| Case B RLAT | -0.63 | 0.89 | -0.50 | 0.13 |
| Case B AP | 0.08 | 1.24 | 0.50 | 0.42 |
| Case B LLAT | -1.00 | 0.97 | -1.30 | -0.30 |
| Case C Pt 3 | 0.91 | 1.26 | -1.10 | -2.01 |
| Case C Pt 5 | 0.34 | 1.28 | -0.80 | -1.14 |
| Case D Pt 3 | -0.23 | 1.10 | -1.20 | -0.97 |
| Case D Pt 5 | 0.58 | 1.42 | -1.20 | -1.78 |
| Case E Avg | -1.73 | 0.53 | -1.72 | 0.01 |
| Case F Avg | -1.65 | 0.87 | -2.80 | -1.15 |
| Case G Avg | -1.29 | 1.27 | -2.22 | -0.92 |
| Case J | 0.02 | 2.23 | -0.20 | -0.22 |
| Case L | -1.38 | 1.44 | -2.10 | -0.72 |

# Discussion

All conformal plans delivered in the audit scored optimal results whether using the HyperSight or FBCT imaging (Fig. 1, Table A2 of the appendix). Five of six delivered modulated cases within the two audits were scored as optimal, with the first audit delivery, Case F, scoring a pass with action level result. The authors propose three contributing factors to the initial case F result which are discussed in detail below.

Although the observed dose difference was small (~ 0.5%) and within typical measurement uncertainty, a trend toward lower calculated doses was observed in beams traversing lung tissue in the HyperSight CBCT-based audit compared with the historic audit distribution. A similar pattern was reported in previous publications [6, 7, 11] and it was evident when comparing HyperSight CBCT– and FBCT-based calculations, suggesting a slight overestimation of lung density in the HyperSight-derived dataset for the phantom scenario. This effect is most evident in the lung SBRT case, where a substantial proportion of beam paths pass through lung-equivalent material.

A slightly elevated linac output, though within tolerance at 0.6%, was observed on the day of the first audit measurement. On the day the subsequent audit was performed the linac output was recorded as within tolerance but cold (-1.0%). This negative output appears to have improved absolute dose results for modulated cases.

This improvement is, in part, due to an offset in calculated dose for modulated cases with respect to conformal fields. This offset is noted for both HyperSight and FBCT calculations in this study, which agree within 0.3%. Figures 2A and 2B demonstrate that dose calculations performed on the HyperSight imaging system fall within the range of measured results from the seven Halcyon linacs previously audited using FBCT-based planning. Historic audit data—calculated using AXB v16.1—show a consistent dosimetry under-reporting of approximately 1.5–2% across all three modulated cases, regardless of whether the scenario is homogeneous or heterogeneous. This systematic underestimation aligns with previously published assessments of modulated dose accuracy on Halcyon systems, indicating a known modelling offset within the Halcyon platform [21, 22]. The introduction of the ELM model in AXB v18.1 appears to have improved, without completely resolving, this model limitation [23].

MLC modelling accuracy is likely to impact the audit results in the SBRT cases, with Miyasaka reporting dose errors as much as 3.5% for highly modulate SBRT deliveries. Cases J and K, both SBRT treatments, successfully passed the audit; however, scored low gamma analysis results 91.2% and 91.0% when considering the 5%/2 mm criteria.

Case L, an SBRT lung target scenario, did not meet the audit criteria in either audit session, with film measurements demonstrating a systematic high measured dose offset with respect to the planning calculation. Strong agreement was observed in geometric localisation and overall dose distribution shape; however, a 5–7% difference in the absolute film dose led to suboptimal gamma analysis outcomes. The microDiamond detector-based measurements show good agreement with the calculated doses in these cases, however, incur substantial measurement uncertainties (approximately ± 10%) as

per Shaw et al [19]. Follow-up investigations of the plan highlighted over-modulation in the case planning. A small but consistent offset was also observed between HyperSight- and FBCT-based calculations for this case. A combination of MLC modelling, small-field model accuracy [21–25] and a slight over-representation of lung density [6, 7, 11] in the HyperSight simulation image are attributed to the out of tolerance results for Case L. Historic audit results for this case suggest that the observed measurement may represent an outlier, and highlight the need for particular care when planning SBRT cases in heterogeneous medium with the Halcyon algorithm.

## Conclusion

A national dosimetry audit was performed using HyperSight CBCT as the primary simulation dataset with all conformal and modulated cases achieving passing results.

A minor difference in reported lung density was observed between HyperSight CBCT and FBCT imaging; however, its dosimetric impact in this audit was minimal, on the order of approximately 0.5%.

The audit highlighted known dosimetry accuracy limitations associated with the Halcyon beam model for small-field, highly modulated stereotactic dose calculation, with extreme caution recommended for implementation of HyperSight imaging for lung SBRT.

Overall, the results indicate that the HyperSight CBCT imaging system provides adequate image quality and Hounsfield unit accuracy to satisfy Australian regulatory requirements for use as a primary simulation imaging modality.

## Declarations

# Conflicts of Interest

This work is in part funded by research agreements between Varian Medical Systems and the authors' institution.

# Author Contribution

Author Contribution StatementBen Archibald-Heeren conceived and designed the project. Peter Phung and Andrew Alves acquired the data. Peter Toth analysed and interpreted the data. Peter Toth wrote, and Maddison Shaw, Peter Pung, Andrew Alves, and Ben Archibald-Heeren reviewed and made additions to the article.

# Acknowledgement

The authors would like to acknowledge Zeyao Li's work on CT/ED tables on HyperSight imaging which was used in this study.

## References

1. Lu L, Zhang Z, Qi P (2024) A review of online adaptive radiation therapy. Appl Radiat Oncol 4. https://doi.org/10.37549/ARO-D-24-00037
2. Radformation I (2026) ChartCheck Adaptive. https://radformation.com/chartcheck/adaptive. Accessed April 09
3. SeeTreat Medical (2026) ART.1. https://www.seetreatmedical.com/art1. Accessed April 09
4. TheraPanacea (2026) https://www.therapanacea.eu/. Accessed April 09
5. Hu Y, Arnesen M, Aland T (2022) Characterization of an advanced cone-beam CT (CBCT) reconstruction algorithm used for dose calculation on Varian Halcyon linear accelerators. Biomed Phys Eng Express 8(2):025023. https://doi.org/10.1088/2057-1976/ac536b
6. Robar JL, Cherpak A, MacDonald RL, Yashayaeva A, McAloney D, McMaster N et al (2024) Novel technology allowing cone beam computed tomography in 6 seconds: A patient study of comparative image quality. Pract Radiat Oncol 14(3):277–286. https://doi.org/10.1016/j.prro.2023.10.014
7. Sijtsema ND et al (2025) Dose calculation accuracy of a new high-performance ring-gantry CBCT imaging system for prostate and lung cancer patients. Radiother Oncol 202:110596. https://doi.org/10.1016/j.radonc.2024.110596
8. Lustermans D et al (2024) Image quality evaluation of a new high-performance ring-gantry cone-beam computed tomography imager. Phys Med Biol 69(10). https://doi.org/10.1088/1361-6560/ad3cb0
9. MacDonald RL et al (2024) The feasibility of CT simulation-free adaptive radiation therapy. J Appl Clin Med Phys 25(9):e14438. https://doi.org/10.1002/acm2.14438
10. Bogowicz M et al (2024) Evaluation of a cone-beam computed tomography system calibrated for accurate radiotherapy dose calculation. Phys Imaging Radiat Oncol 29:100566. https://doi.org/10.1016/j.phro.2024.100566
11. Haertter A et al (2024) ACR benchmark testing of a novel high-speed ring-gantry linac kV-CBCT system. J Appl Clin Med Phys 25(5):e14299. https://doi.org/10.1002/acm2.14299
12. Zhao H et al (2024) Comprehensive image quality evaluation and motion phantom studies of an ultra-fast (6-second) cone-beam computed tomography imaging system on a ring gantry linear accelerator. Adv Radiat Oncol 10(2):101681. https://doi.org/10.1016/j.adro.2024.101681
13. Kunnen B et al (2024) The added value of a new high-performance ring-gantry CBCT imaging system for prostate cancer patients. Radiother Oncol 200:110458. https://doi.org/10.1016/j.radonc.2024.110458
14. Australian Radiation Protection and Nuclear Safety Agency (ARPANSA). ACDS audit program. October 2023. Accessed April 09 (2026)

https://www.arpansa.gov.au/sites/default/files/documents/2023-10/ACDS%20audit%20program%20OCT%202023%20-%20Digital.pdf

15. Sun Nuclear Corporation. E2E SBRT Phantom with Removable Spine, Model 036S datasheet (036S-PB-071921-2). Accessed April 09 (2026) https://www.sunnuclear.com/uploads/documents/datasheets/036S-PB-071921-2.pdf
16. Lehmann J et al (2018) Dosimetric end-to-end tests in a national audit of 3D conformal radiotherapy. Phys Imaging Radiat Oncol 6:5–11. https://doi.org/10.1016/j.phro.2018.03.006
17. Australian Radiation Protection and Nuclear Safety Agency (ARPANSA) (2026) Level III audit fact sheet (ARPANSA-SUP-3002). https://www.arpansa.gov.au/sites/default/files/arpansa-sup-3002_l3_fact_sheet.pdf. Accessed April 09
18. Kry SF, AAPM Task Group 329 et al (2020) Reference dose specification for dose calculations: Dose-to-water or dose-to-muscle? Med Phys 47(3):e52–e64. https://doi.org/10.1002/mp.13995
19. Shaw M et al (2021) Characterisation of a synthetic diamond detector for end-to-end dosimetry in stereotactic body radiotherapy and radiosurgery. Phys Imaging Radiat Oncol 20:40–45. https://doi.org/10.1016/j.phro.2021.10.002
20. Shaw M et al (2025) Comprehensive end-to-end dosimetry audit for stereotactic body radiotherapy in spine, lung, and soft tissue. J Appl Clin Med Phys 26:e70133. https://doi.org/10.1002/acm2.70133
21. Hernandez V et al (2021) Dosimetric leaf gap and leaf trailing effect in a double-stacked multileaf collimator. Med Phys 48(7):3413–3424. https://doi.org/10.1002/mp.14914
22. Miyasaka R, Cho S, Hiraoka T et al (2022) Investigation of Halcyon multi-leaf collimator model in Eclipse treatment planning system: A focus on VMAT dose calculation with the Acuros XB algorithm. J Appl Clin Med Phys 23(3):e13519. https://doi.org/10.1002/acm2.13519
23. Miyasaka R et al (2025) Commissioning of Halcyon enhanced leaf model in the Eclipse treatment planning system: Focus on simple slit fields and VMAT dose calculation. J Appl Clin Med Phys 26(6):e70044. https://doi.org/10.1002/acm2.70044
24. Hu Y et al (2020) Validation of the preconfigured Varian Ethos Acuros XB beam model for treatment planning dose calculations: A dosimetric study. J Appl Clin Med Phys 21(12):27–42. https://doi.org/10.1002/acm2.13056
25. Fogliata A, Stravato A, Dusi F et al (2026) Small field dosimetry on a ring-shape linac machine with a dual-layer MLC. Med Phys 53:e70310. https://doi.org/10.1002/mp.70310

# Figures

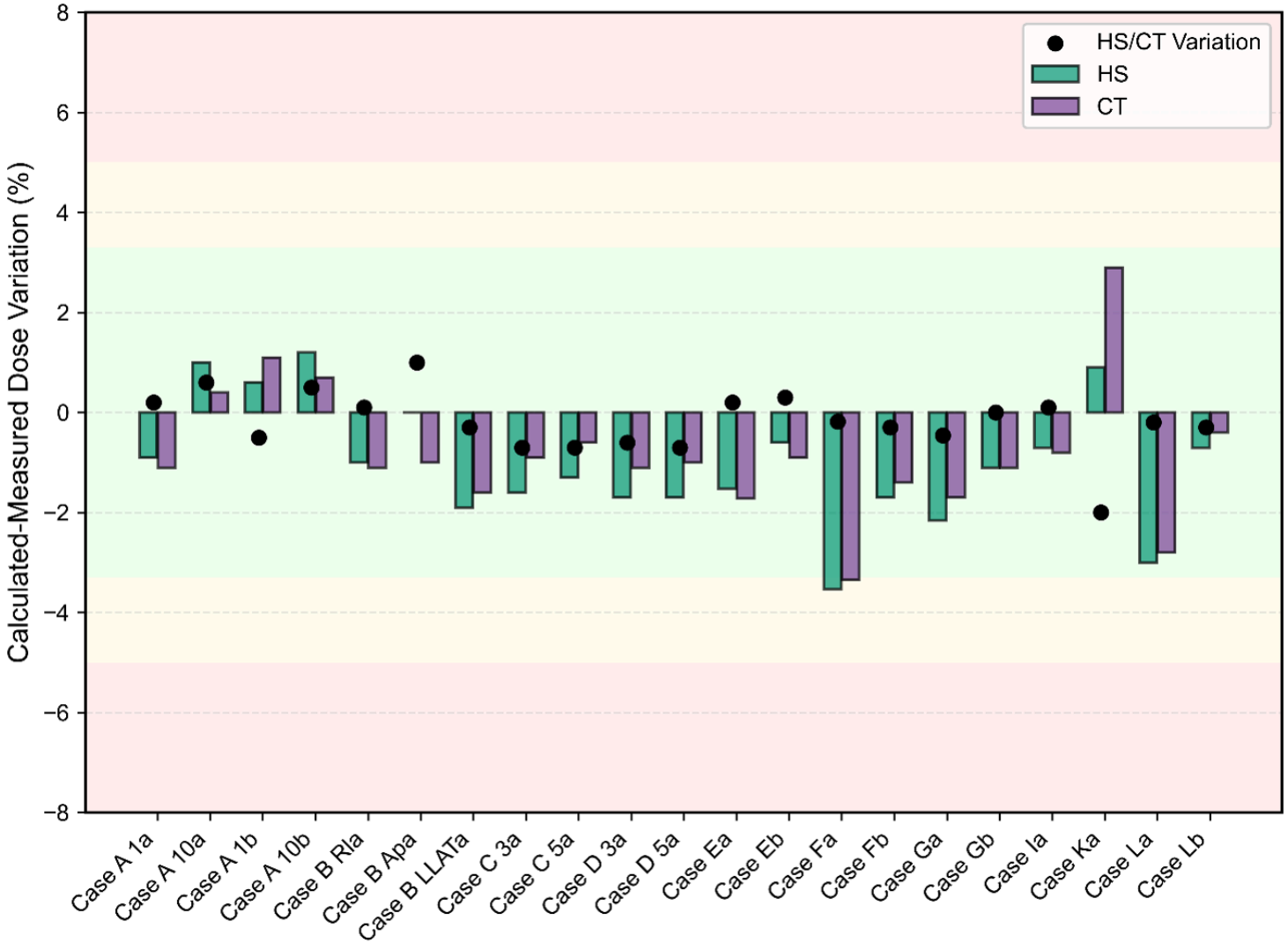



**Figure 1**

HyperSight CBCT (HS), FBCT (CT) measured chamber audit results, and calculated dose variation for conformal cases (Case A- Case D), modulated cases (Case E-G), and stereotactic deliveries (Cases J-L). Initial measurements are denoted with suffix (a) and repeat measurements (b)

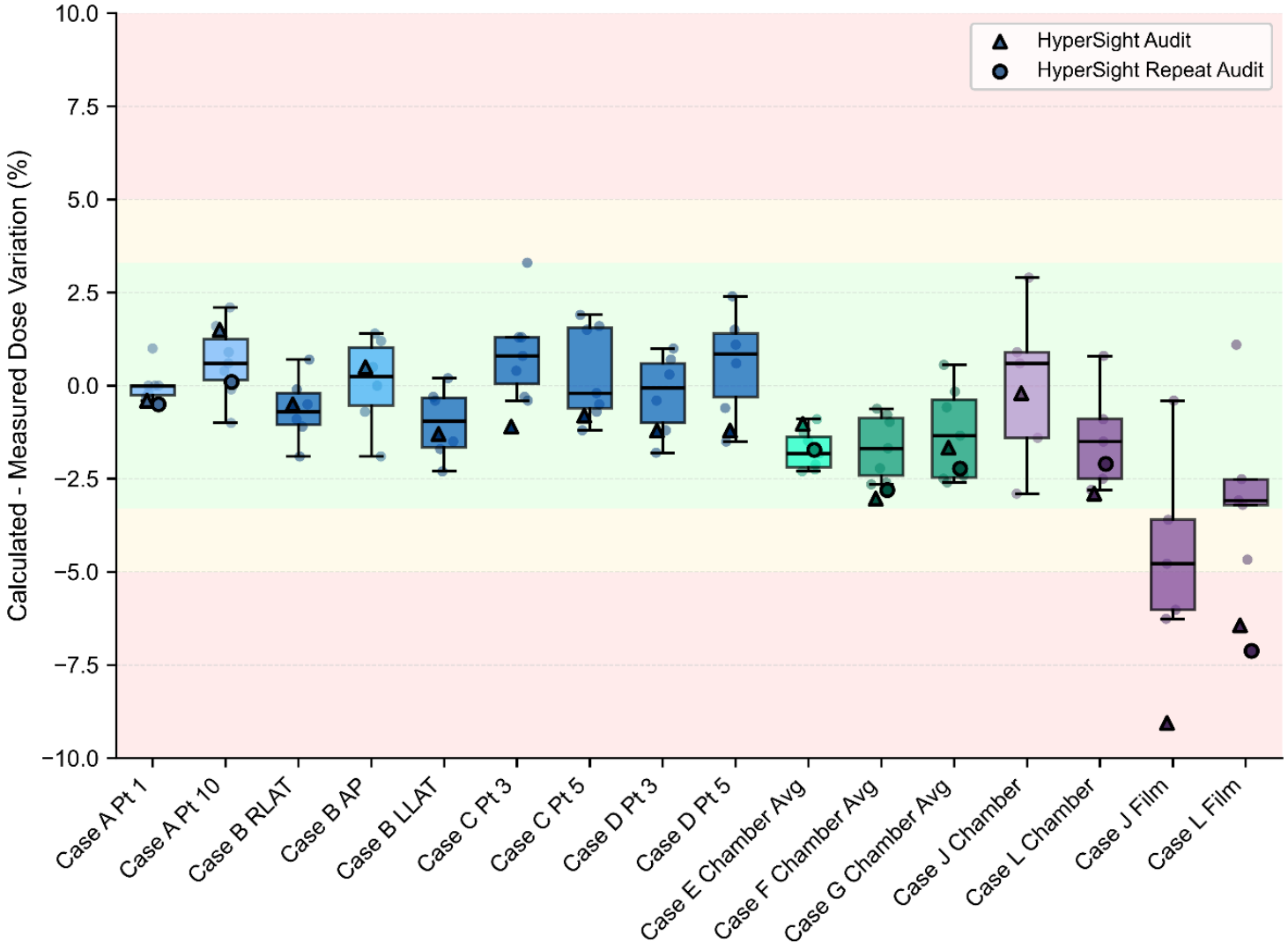



**Figure 2**

Case comparison of 7 Halcyons and the HyperSight audit for conformal (blue), modulated (green) and SBRT (purple) deliveries. Deliveries to homogeneous and heterogeneous scenarios are distinguished with light and dark shades. Note that C) includes measurements with the microDiamond and film detectors.

## Supplementary Files

This is a list of supplementary files associated with this preprint. Click to download.

- Appendix.docx